Article:
Zaki, M., Rajkhowa, R., Holland, C. et al. (2025) Anions, not cations, drive silk stability and self-assembly: insights from regenerated undegummed silk. ACS Biomaterials Science & Engineering, 11 (9). pp. 5285-5292. ISSN: 2373-9878

https://doi.org/10.1021/acsbiomaterials.5c01113

Title

Anions, not cations, drive silk stability and self-assembly: Insights from Regenerated Undegummed Silk

Authors and Affiliations

Martin Zaki[1], Rangam Rajkhowa[1], C. Holland[2], Joselito M. Razal[1], Dylan Y. Hegh[1], Benjamin J. Allardyce[1]

Corresponding Author- ben.allardyce@deakin.edu.au

[1] Institute for Frontier Materials, Deakin University, Geelong Waurn Ponds Campus, Pigdons Road, Geelong, VIC-3216, Australia

[2] School of Chemical, Materials and Biological Engineering, University of Sheffield, Sir Robert Hadfield Building, Mappin Street, Sheffield S1 3JD, U.K

Abstract

The self-assembly of β-sheet rich proteins such as silk are triggered by physiochemical factors such as salts, pH, and flow. Anions in particular have been shown to significantly influence protein self-assembly in amyloids and spider silk, however their effect on silkworm silk has not yet been investigated. This study evaluated the influence of metal ions on silk gelation kinetics by utilising a recently developed system to dissolve undegummed *B. mori* cocoons. While the influence of cations agreed with previous observations, with divalent cations delaying gelation more than monovalent ions, we report that anions are more influential, with phosphate and sulphate anions accelerating gelation, regardless of the valency of the associated cation, while bromide was found to delay it. Interestingly we discovered chloride stabilised silk regardless of the cation. Using these results, a linear relationship was established between gelation time and apparent dynamic hydration number, a quantitative measure of salt-water interactions. This relationship more accurately predicted silk behaviour than the traditionally used Hofmeister series. Thus, it was possible to accurately predict gelation behaviour for any salt for which this number has been calculated, allowing for better designs of systems that require fine control of gelation such as wet-spinning and 3D printing This work demonstrates the significance of anions in controlling silkworm silk stability, expanding upon the currently perceived mechanism for self-assembly.

Keywords

Silk, fibroin, sericin, biomimetic, composite materials, biomaterials, gelation stability, metal ions,

1. Introduction

Silkworm silks are among the toughest fibres found in nature. Yet, the exact mechanism underlying fibre formation is not completely understood. The self-assembly of the silk solution into a hierarchical fibre is a complex physiochemical transition. The role of pH,[1-3] metal salt cations,[3-9] temperature,[9] and flow are now beginning to be understood.[6, 10, 11] Several metal cations have been identified within the gland, with potassium, sodium, calcium and magnesium being most prevalent.[4, 5, 8, 12] Divalent cations such as calcium and magnesium are believed to stabilise native silk fibroin feedstock and prevent premature aggregation during the early stages of silk production.[3] This stabilisation is thought to occur through the formation of carboxylate mediated salt bridges,[4, 13, 14] preventing β-sheet formation.[3] As silk migrates down the gland duct, the concentration of monovalent cations such as potassium and sodium increases. These displace the divalent cations, disrupting the salt bridges and facilitating β-sheet formation.[4, 9] It is therefore believed that cations play a role both in the initial stages of silk protein production and during the final spinning process.

However, the role of anions in silkworm silk's structural transitions are less explored. Sulphur, phosphorous and chlorine have been identified within silk dissected from the gland using Inductively Coupled Plasma Optical Emission Spectroscopy and Energy Dispersive Spectroscopy.[7, 8] However, these techniques cannot distinguish between individual elements and molecules composed of several elements. It has therefore been difficult to differentiate between sulphur chelating with silk and sulphur present within fibroin amino acids (Cys, and

Met) and the disulphide link between heavy and light chains. Similarly, identification of free phosphate anions in the gland is challenging since phosphorylation plays several roles broadly in Lepidopterans such as regulating the metabolism,[15] immune response,[16] and also silk production.[17, 18] Phosphate is involved in fibroin synthesis and secretion from the posterior gland,[17] but are also thought to have a role in fibre self-assembly at the anterior.[18, 19] On the other hand, pH is enzymatically regulated by the secretion of carbonic anhydrase by type IV epithelial cells,[1, 2, 20] leading to the progressive acidification of the gland lumen between the posterior and anterior gland.[20] While alkaline conditions have been shown to stabilise silk,[3, 21] a decrease in pH along the spinning gland is believed to initiate fibre formation.[22] However, the role of pH is usually studied using a metal salt buffer, such as phosphate[21, 23, 24], and it is therefore unclear whether these metal salts contribute to changes in silk solubility in a way that does not reflect naturally occurring conditions in the gland. Therefore, to remove the influence of metal salts, pH should be evaluated using a range of metal salts, ideally a salt pair that induces gelation and one that delays gelation.

The effect of cations and anions on proteins is commonly understood through the Hofmeister series, which ranks the ions for their ability to alter the proteins solvency.[25] Originally, the Hofmeister series was determined experimentally using serum globulin and albumin proteins.[25] Model polymers such as poly(N-isopropylacrylamide) (PNIPAM) were then used to further understand the series.[26] Anions were found to bind directly to the PNIPAM side-chain moieties, and polarise water molecules hydrating the polymer, raising the surface tension at the polymer/water interface. While the paired cation also influences solvency, the anion has been found to be more influential due to their specific radial charge densities, ion solvation, and ion polarizability.[27-30] Although anions have been explored in both model polymers and well-characterized natural silks, such as spider major ampullate silk,[31-33] these systems differ markedly from silkworm silk. In addition to significant differences in amino acid sequences,

81 silkworm silk comprises a far more complex protein mixture (over 200 proteins),[34] which may
82 complicate the self-assembly process. To better understand silkworm silk-ion interactions,
83 experimental data evaluating several salt pairs is required to establish the relationship between
84 metal ions and silk stability.

85 This study therefore aimed to understand the relative importance of cations, anions and pH to
86 the stability of silkworm silk by incubating silk solutions with a range of salts and at different
87 pHs. Regenerated, undegummed silk (RUS) solution recently developed by our group was
88 utilised since it more closely resembles molecular weight and composition of silk as it is spun
89 compared with degummed, regenerated silk.[35] Gelation times in these different environments
90 were measured through monitoring changes in turbidity. Finally, the results of this work were
91 used to build a complete picture of the relative roles of these variables, enabling the prediction
92 of the effect of any combination of anion and cation. This work not only expands on current
93 understanding of silkworm silk self-assembly but will guide the design of spinning dopes and
94 baths to produce superior artificial fibres.

95

96 **2. Materials and methods**

97 **2.1. Chemicals and materials**

98 Bivoltine *Bombyx mori* (*B. mori*) reeled, undegummed fibres were purchased from an SRR
99 Silk Reeling Unit (Ramanagara, Karnataka, India) and cut into 2 mm pieces using a Pulverisette
100 25 power cutter mill (Fritsch, Idar-Oberstein, Germany). The salts lithium bromide (LiBr,
101 99%), sodium carbonate (Na_2CO_3, 99.5%), sodium hydroxide (NaOH), lithium chloride (LiCl),
102 sodium chloride (NaCl), calcium chloride ($CaCl_2$), calcium hydroxide ($CaOH_2$), calcium
103 carbonate ($CaCO_3$), magnesium chloride ($MgCl_2$), magnesium hydroxide ($MgOH_2$),

magnesium sulphate ($MgSO_4$), potassium chloride (KCl), potassium bromide (KBr), potassium hydroxide (KOH), potassium phosphate monobasic (KH_2PO_4), potassium phosphate dibasic (K_2HPO_4), and acids hydrochloric acid (HCl), sulphuric acid (H_2SO_4) were purchased from Sigma-Aldrich (St Louis, MO, USA).

2.2. Sodium carbonate degumming of B. mori silk

Na_2CO_3 degumming was done using a previously described method.[35] Briefly, *B. mori* silk fibers were degummed using 500 mL aluminum pots in an Ahiba IR Pro rotary dyeing machine (Datacolor, Lawrenceville, USA) with a raw silk (g): liquor (ml) ratio of 1:50. Raw silk was degummed for 30 minutes at 98 °C using 0.2% (w/v) Na_2CO_3. A weight loss of 28.5% (w/w) was calculated using the dry weights before and after degumming.[36]

2.3. Preparation of Regenerated Silk solutions

Regenerated silk solutions were prepared using a previously described method, with minor modifications.[35] Briefly, degummed and raw silk was dissolved in 9.3 M LiBr solution with a silk (g): liquor (ml) ratio of 1:16 at 60 °C for 4 hours. The solutions were dialysed using 3.5 kDa dialysis tubing in a custom-made flowing deionised water bath for 2 days at 4 °C. To remove insoluble fractions, solutions were centrifuged twice at 7000 RCF for 10 minutes at 4 °C. Regenerated silk solutions were concentrated using a modified version of previously described methods,[37, 38] briefly, solution was added to 3.5 kDa dialysis tubing and left to dry against air in a fume hood, with the aid of a small fan, leading to gradual increase in concentration. The concentration (w/w) was calculated gravimetrically by drying 1g at 60 °C for a minimum of 5 hours and weighing the dried film.

A matrix of silk solutions containing different concentrations of metal ions at different pHs were prepared by diluting 12% (w/w) stock silk solution with different volumes of 2 M aqueous salt solution to achieve final concentrations of 100 and 200 mM salt with 10% silk. Previous studies have shown that concentration influences the gelation kinetics of RUS.[35] Increasing the concentration above 15% inhibited gelation, while below 5% RUS gelled quickly. Therefore, a concentration of 10% was selected to maintain an optimal gelation rate. Prior to dosing, all salt solutions were sterilised at 121 °C for 45 minutes using an Tomy SX-700E Toploading Autoclave (Bio-Strategy, Tullamarine, Victoria) to minimise microorganism contamination. Different cations, anions and pH were evaluated. To evaluate the role of various ions, salt solutions were buffered to pH 7 to eliminate pH effects on silk (**Table 1**). pH adjustment was achieved using different methods, depending on the salt. Phosphate salt solutions were buffered by adjusting the amount of monobasic (KH_2PO_4) and dibasic (K_2HPO_4) salt. Depending on the pH, phosphate buffer consists of either more $H_2PO_4^-$ or HPO_4^{2-}. Therefore, phosphate reported in this study relates to $H_2PO_4^- \rightleftharpoons HPO_4^{2-}$. To maintain simplicity throughout, potassium phosphate has been reported as K_3PO_4. Chloride and bromide solutions were altered with 10mM HCl or the respective hydroxide salt. Sulphate salt solutions were altered using 10mM of the respective metal hydroxide and sulphuric acid. Due to the poor solubility, the only divalent-polyanion evaluated was magnesium sulphate.

Conversely, to evaluate the effects of pH, 100 mM KCl and K_3PO_4 buffered to pH range in the gland (5, 6, 7, and 8) were dosed into 10% RUS solution.[1, 20, 39] However, 100mM K_3PO_4 at pH5 instantly gelled silk after addition and could not be further evaluated.

Table 1. Acids and Bases used to adjust pH of the salts in this study

Salt	Acid	Base
KCl	HCl	KOH

NaCl	HCl	NaOH
$MgCl_2$	HCl	$MgOH_2$
$CaCl_2$	HCl	$CaOH_2$
KBr	HCl	KOH
K_2SO_4	H_2SO_4	KOH
K_3PO_4	KH_2PO_4	K_2HPO_4
$MgSO_4$	H_2SO_4	$MgOH_2$

148

149 **2.4. Molecular weight distribution**

150 The molecular weight was evaluated with Sodium dodecyl sulphate polyacrylamide gel
151 electrophoresis (SDS-PAGE) based on the Laemmli method,[40] and using an Invitrogen Mini
152 gel tank (ThermoFisher, Waltham, MA, USA) coupled with a PowerPac Basic power supply
153 (Bio-Rad, Hercules, CA, USA). 30 µg of protein and 10 µl of ~~each~~molecular protein ladder
154 (Novex Sharp Prestained Protein Standard) was loaded onto a NuPAGE 4-12% Bis-Tris gel.
155 To improve separation at low SDS concentration gradients and prevent overheating,
156 electrophoresis was undertaken with a stepped increase in voltage of 80 V for 20 minutes and
157 then 100 V for 50 minutes, followed by 150 V for 20 minutes.[41] The resulting gel was stained
158 using a Colloidal blue staining kit for 3 hours, de-stained overnight in Milli-Q water, and
159 imaged using a gel imaging system (ChemiDoc XRS+, Bio-Rad, Hercules, CA, USA). Gel
160 analysis was performed using Origins Gel Molecular Weight Analyzer to determine the MW
161 of the bands observed.[42] All SDS-PAGE consumables were obtained from ThermoFisher
162 (Waltham, MA, USA).

163 **2.5. Gelation kinetics**

164 Gelation kinetics were evaluated using a previously reported method with minor
165 modifications.[23] Briefly, silk solutions at different concentrations were evaluated in covered
166 96-well plates. A 300 µL aliquot of solution was gently pipetted into each well to avoid
167 premature shear-induced gelation. To limit fluctuations at ambient conditions, the lid was

sealed onto the plate with parafilm, and the samples were stored light-free at 30 °C in an incubator (HeraCell 150i, ThermoFisher Scientific, Waltham, MA, USA). Turbidity changes at 550 nm were monitored with a Varioskan LUX microplate reader (ThermoFisher Scientific, Waltham, MA, USA). Each variable was dosed in triplicate and Standard deviation reported as the shadow. All stability figures reported in the main text were normalised. Original figures are available in the SI (**Supporting Figure 4**)

2.6. Analysis of Precipitate

Fourier Transform Infrared (FTIR) Spectroscopy was utilised to identify the precipitate formed when calcium chloride was added to RUS solution. The precipitate was washed thoroughly with deionised water and then dried at 60 °C. Additionally, salt-free RUS solution was cast into a film at 60 °C. FTIR spectra were measured using a Bruker LUMOS II FTIR microscope (Billerica, MA, USA) equipped with a Germanium ATR crystal. Spectra were scanned over the range of 4000 – 600 cm^{-1} with a resolution of 2 cm^{-1} and 128 scans per sample.

3. Results and discussion

This study utilised regenerated undegummed silk (RUS), a recently reported ~~new~~ class of regenerated silk solution.[35] Physiochemical parameters are usually evaluated using either native fibroin dissected directly from the gland (native silk fibroin, NSF) or regenerated silk fibroin (RSF). Extracting gland protein is the most reliable way to obtain intact (undegraded) silk and gives direct insight to the concentration of metal ions and pH at a given section of the gland. The effect of sodium chloride and potassium chloride on the gelation kinetics of dilute NSF (0.1%) has been previously investigated.[9] Increasing the salt concentration from 2.3% to 8.4% reduced the temperature required to induce turbidity of gland silk. At these concentrations, the salts were thought to reduce water's chemical affinity to the silk proteins,

thereby promoting gelation. However, the tested salt concentrations were higher than those typically found in the gland.[4, 5, 12] On the other hand, RSF can be effectively dialysed to analyse the roles of individual metals. To produce RSF, silk must first be degummed, a process that removes sericin and improves the solubility of fibroin. However, degumming may hydrolyse the proteins,[36, 43, 44] impacting and increasing the distribution of the effective molecular weight between chemical entanglements and increase the free volume and thus mobility of the system which could lead to unreliable measurements.[11, 45, 46] Therefore, it is difficult to separate the effect of metal ions from the influence of protein degradation. Recent work by our group has developed a method to dissolve silk from *Bombyx mori* (*B.mori*) cocoons without degumming. The resulting RUS solution maintains the molecular weight of silk without removing sericin, making it an excellent model to evaluate the influence of cations, anions and pH.[35]

3.1. Cations

The influence of cations on silk gelation kinetics was evaluated by dosing 100 and 200 mM metal chloride salts into 10% RUS at pH 7 (**Figure 1**), mimicking the upper salt concentration limit in the silk gland (**Supporting Table 1**).[4] When incubated in a sealed, dark microwell at 30 °C, salt-free silk solution gelled within 19 days. The addition of chloride, regardless of the cation present or concentration, delayed gelation. At 100 mM, the gelation times ranged from 21 days for sodium chloride to 37 days for magnesium chloride. This effect was more pronounced at 200 mM, with the sodium chloride silk sample gelling 23 days later, while the 200 mM magnesium chloride sample did not gel at all over the 45-day incubation period. Surprisingly, when calcium chloride was added to RUS, precipitate formed, which likely led to the observed increase in turbidity for the baseline. Upon further inspection, the precipitate corresponded to the formation of calcium carbonate that likely formed when absorbed atmospheric CO_2 displaced chloride ions within the solution (**Supporting Figure 2**).[47] The formation of calcium carbonate would decrease the availability of free calcium, which in turn

diminishes its ability to delay silk gelation. However, the baseline levels for both the 100 mM and 200 mM solutions were similar, suggesting that calcium carbonate production is limited and that the 200 mM calcium chloride solution contains an additional 100 mM of free calcium. Overall, monovalent cations, sodium and potassium, were less effective than the divalent cations, calcium and magnesium with general stability organised in the following order:

$$\text{No Salts} < \text{NaCl} < \text{KCl} < \text{CaCl}_2 < \text{MgCl}_2.$$

This effect observed for divalent cations aligns with previous findings, where calcium delays gelation more than potassium in RSF.[48] During the early stages of silk production, calcium is believed to stabilise the concentrated solution through formation of salt bridges,[4, 6, 13, 14] preventing premature aggregation. As silk migrates along the gland duct, the monovalent ions compete with divalent ions, disrupting the salt bridges and random coil interactions, allowing the silk to move freely which in turn enables the formation of β-sheets. Our observations are generally in line with this theory: divalent cations delayed the gelation more effectively than monovalent cations. However, monovalent ions still delayed the gelation, suggesting the chloride anion may contribute to silk stability via specific attractive charge-charge interactions.

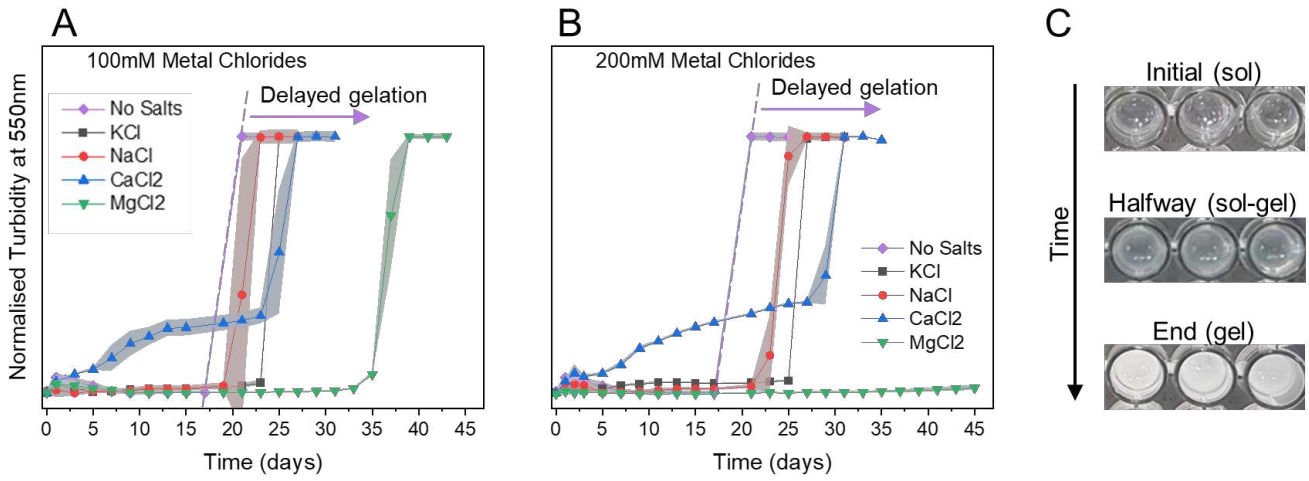

Figure 1. Cation influence on silk gelation kinetics. Turbidity measurements over time for 10% RUS solution at pH 7 with various metal chloride salts dosed at A) 100 mM and B) 200 mM.

Where Y_{error} = ± SD is represented in by the shaded regions, and n = 3. C) Macroscopic images illustrating the typical transition of solution to a gel for all silk solutions studied.

3.2. Anions

To quantify the influence of chloride on delaying silk gelation, the effect of anions was explored by evaluating potassium salts with varying anions (**Figure 2A** and **2B**). The choice of anions significantly altered the gelation profile of silk. Polyvalent phosphate and sulphate anions accelerated the gelation rate, while monovalent chloride and bromide anions delayed gelation time, with 200 mM bromide completely preventing gelation throughout the entire test. To ensure the cation valency did not alter anion behaviour, magnesium sulphate and chloride were also evaluated (**Figure 2C** and **2D**). Magnesium chloride was the most effective metal chloride in delaying gelation, while magnesium sulphate significantly accelerated the gelation. Overall, these comparisons strongly indicate that anions drive the changes in solubility of silk more strongly than cations. Salts which contained the same anion (for example potassium sulphate vs magnesium sulphate) had very similar gelation times (15 days for potassium phosphate and 17 days for magnesium sulphate). In contrast when keeping the cation consistent, but changing the anion (for example magnesium chloride vs magnesium sulphate) the gelation behaviour changed significantly (37 days for magnesium chloride and 17 days for magnesium sulphate). Whilst our turbidity measurements clearly demonstrate the impact of anion/cation pairs on bulk gelation, future studies are planned to dive deeper into this area and explore this systems gelation kinetics in more detail.[9, 23, 49-51]

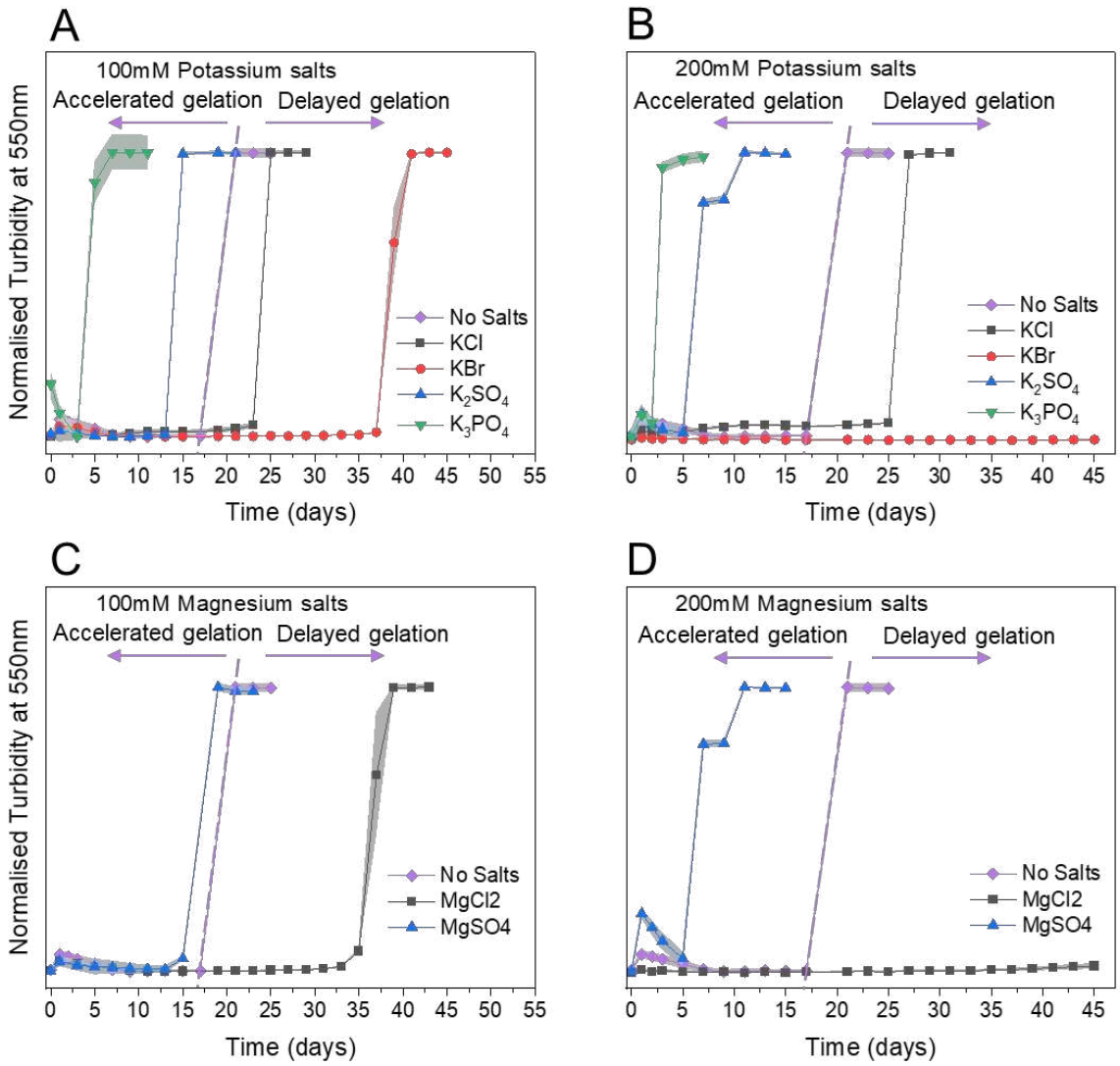

Figure 2. Anion influence of silk gelation kinetics. Turbidity measurements over time for 10% RUS solution at pH 7 with various potassium (A and B) and magnesium (C and D) salts dosed at 100 mM and 200 mM. Where Y_{error} = ± SD is represented in by the shaded regions, and n = 3.

3.3. Influence of pH, sericin, and molecular weight

To identify whether pH significantly altered the influence of salts, silk gelation was tested using 100 mM potassium chloride and potassium phosphate at pH 5, 6, 7, and 8 (**Figure 3**). The silk solution containing potassium phosphate at pH 5 gelled almost instantly and therefore could not be evaluated. For both salts, decreasing the pH, decreased gelation time. This trend agrees with literature, as acidification is well known to induce gelation of silk.[3] Increasing the pH of

potassium chloride from 7 to 8 by adding potassium hydroxide delayed gelation, with pH 7 solution gelling at 20 days and pH 8 at 30 days, delaying gelation by an additional 10 days. However, all phosphate-containing solutions regardless of pH gelled earlier than the solution with no salts, indicating that salt, especially phosphate, can be as influential as pH. From these results, we suggest that future pH studies evaluate potassium chloride (adjusted with KOH and HCl) alongside their buffer.

Degummed silk fibroin was also tested with several salts to ensure that sericin and molecular weight did not modify the salts interaction with fibroin (**Supporting Figure 1** and **3).** The gelation profiles of the degummed silk with different salts closely matches undegummed silk, indicating that sericin does not significantly alter how the ions interact with silk fibroin in solution. As for RUS, chlorides delayed gelation, with divalent cations having a stronger influence, while phosphate induced gelation. Therefore, it is unlikely that sericin significantly alters the ion influence on the silk fibroin sol-gel transition at the tested salt concentration.

Interestingly, RSF presented a slower gelation rate compared to RUS. For instance, RSF with 100 mM potassium chloride gelled over the course of 12 days, whereas RUS under the same conditions gelled in just 2 days. Variation can be influenced by microorganisms and thermodynamic factors, such as entropy and temperature.[9, 52] However, temperature was kept constant and samples were sterilised prior to testing and are unlikely to have influenced this study. Solubility typically decreases with increasing molecular weight. RUS, with its higher molecular weight, more readily forms hydrogel networks due to its enhanced capacity for chain entanglement, physical crosslinking, and Van der Waal interactions leading to the observed faster gelation rate compared to RSF.[11, 45, 46]

Additionally, polymer concentration plays a critical role. As shown in a previous study, increasing polymer concentration reduced gelation time.[23] This is likely due to the availability

of additional interactive sites within the system which promotes network formation.[53, 54] Contrary to pure RSF, increasing RUS concentration was previously found to increase gelation time,[35] with sericin likely contributing to the delay in gelation time.[54] Although the overall concentration was constant, degummed RSF contained a higher proportion of fibroin than the sericin-rich, undegummed RUS. Based on fibroin content, RSF would be expected to gel earlier, especially as sericin has been reported to have a stabilizing effect.[54] However, both solutions finished gelling at similar times and shifted depending on the salt, indicating that salt type is the dominant factor in gelation at the polymer concentrations tested. Additionally, it is possible that the two systems (RSF and RUS) may behave differently at varying polymer concentrations, which will be explored in future work.

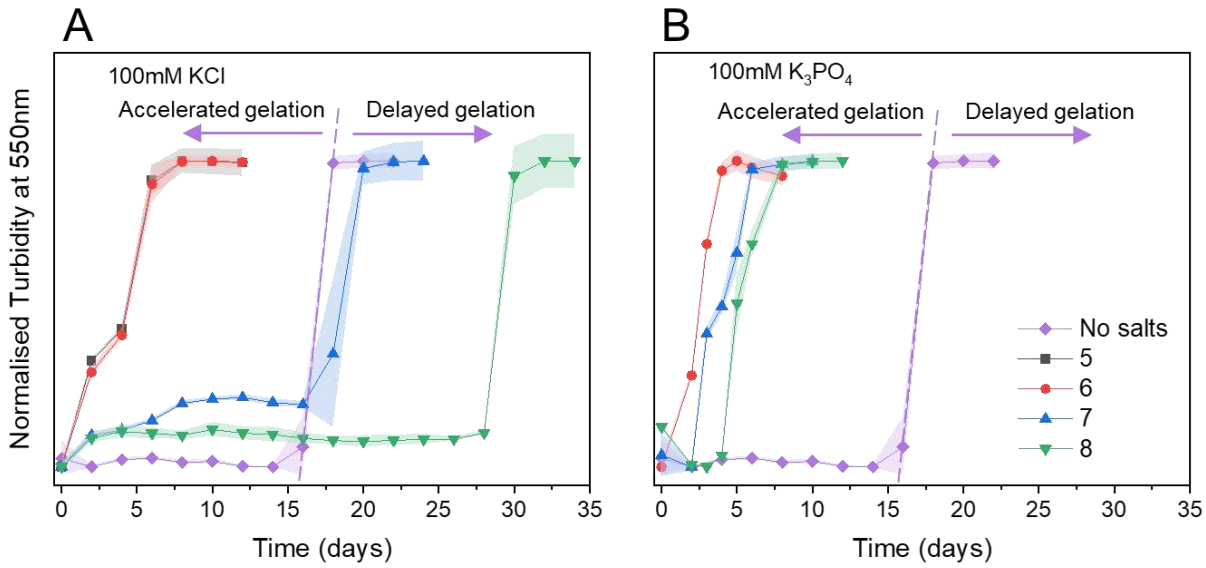

Figure 2. Influence of pH on silk gelation kinetics. Turbidity measurements over time for 10% RUS solution at varying pH using A) 100 mM KCl adjusted with HCl and KOH and B)100 mM K_3PO_4 buffer. Where $Y_{error} = \pm$ SD is represented in by the shaded regions, and n = 3.

3.4. Correlating gelation time with metal ions

The stability profiles of the different salts in this study closely match the Hofmeister series.[25] The series categorises ions by their ability to improve or reduce protein solubility depending on how the ion interacts with both water and the protein.[29] While it was originally developed using model proteins (albumin and serum globulin),[25] this series is widely accepted as a starting point to predict solubility of many proteins, including silk.[30, 31, 55, 56]

Based on the Hofmeister series, one would expect bromide, nitrate, and thiocyanate anions to significantly delay gelation and effectively dissolve silk and in fact, this is the case in practice for silk.[57-59] Similarly, the Hofmeister series predicts that citrate, phosphate, and sulphate promote solidification. As expected, these anions do decrease silk solubility and are therefore commonly used as coagulants in spinning baths.[37, 60] Furthermore, in spider silk, chloride alongside divalent cations hypothetically prevents gelation during silk storage, while phosphate triggers the solidification into a fibre.[61]

However, while useful, the Hofmeister series ranks anions and cations separately, making it challenging to understand the behaviour of the salt as a whole. Therefore, this study proposes an alternative approach that utilises a calculated value for each salt referred to as the apparent dynamic hydration number (ADHN). ADHN was proposed as a quantitative method to explain how water binds to ions through measuring their retention time when run through a Sephadex® G-10 size exclusion chromatography column (**Supporting Table 2**).[62, 63] ADHN was calculated using the apparent molecular weight for a neutral salt, and the excess molecular weight (in the form of tightly bound water molecules) obtained through the column. As the ADHN of cations did not differ when determined with either chloride or formate salts, it was concluded that the ADHN of strongly hydrated ions does not depend on the counter ion. This means that weakly hydrating ions such as K^+ and Cl^- do not influence their counter parts and ADHN for individual ionic species could be defined. However, it also highlights the limitation

to this approach: when there are two strongly hydrating ions. Unfortunately, experimental values for these salts have not been explored yet. Additionally, ADHN differs from hydration number where the total number of water molecules are considered to be part of the hydration shell but rather the number that are strongly enough associated to behave as part of the diffusing entity. For example, Cl^- has a hydration number of 6, but has a ADHN of 0, indicating that no water molecules are tightly bound to Cl^-. This previous work highlighted the importance of the hydrated size of the salt in driving interactions in biological environments.

The present study builds on this work; here, we have adapted ADHN by assigning a negative value to anion-dominant salts (**Supporting Table 3)**. Considering salt pairs as cations and anions competing for water offers a more complete understanding. At a positive ADHN, the cation is strongly hydrated and the anion weakly hydrated; conversely, at a negative ADHN, the cation is weakly hydrated while the anion is strongly hydrated. This enables the gelation times of different salts (100mM) to be plotted against their literature ADHN **(Figure 4B**). Remarkably, this plot produced a strong linear relationship for silk gelation (R^2=0.98). Using this newly discovered relationship, it is possible to predict the gelation time for any salt which has a calculated ADHN. To demonstrate, 5 additional salts were plotted against the trendline, leading to predicted gelation times ranging from 5 days (for potassium fluoride) to more than 45 days (for chromium (III) chloride, **Figure 4B**). While trivalent cations may complex with certain functional moieties, they are unlikely to have a significant influence on the gelation kinetics due to their low solubility and slow diffusion.[64, 65] Furthermore, this relationship can be combined with the Hofmeister series to evaluate the influence of anions and cations alongside the whole salt pair (**Figure 4A** and **4C**). We propose that the order of anions presented in the Hofmeister series is useful to determine the effective range for gelation time and beyond that, the ADHN trend can be used to determine variations within this range based on the cation used. Just as the trendline can been used to predict gelation times of untested

356 salts, the experimental values of gelation time can be used to predict the ADHN of salts. For
357 example, extrapolating the gelation time for $MgSO_4$ would provide a ADHN value of ~ -1.5,
358 indicating that SO_4^{2-} is more strongly hydrated than Mg^{2+}.

359 While promising, the final step in validating this model would ideally be to experimentally
360 measure gelation time for these salts and compare with the predicted times. However, it was
361 not possible to do this. Aluminium, chromium, and zinc have limited solubility at pH 7, and
362 potassium fluoride potentially forms hydrofluoric acid, which could chemically alter the silk
363 proteins (**Supporting Table 3**). Beyond this, the ADHN for other salts have not been published
364 so cannot be plotted against the trendline.

365 ADHN is not widely used in protein solubility studies, but this work demonstrates that there
366 may be value in screening more salts such as lithium bromide, ammonium sulphate, and
367 calcium nitrate using this method. We anticipate that lithium bromide would act similarly to
368 potassium bromide, exhibiting a high positive ADHN and consequently delaying gelation. In
369 fact, highly concentrated lithium bromide solutions are frequently used to dissolve silk.[35, 66]
370 Conversely, ammonium sulphate would exhibit a negative ADHN and is expected to resemble
371 potassium and magnesium sulphate, and thereby promotes silk gelation. Likewise, ammonium
372 sulphate is widely used for protein precipitation.[37, 59, 67]

373

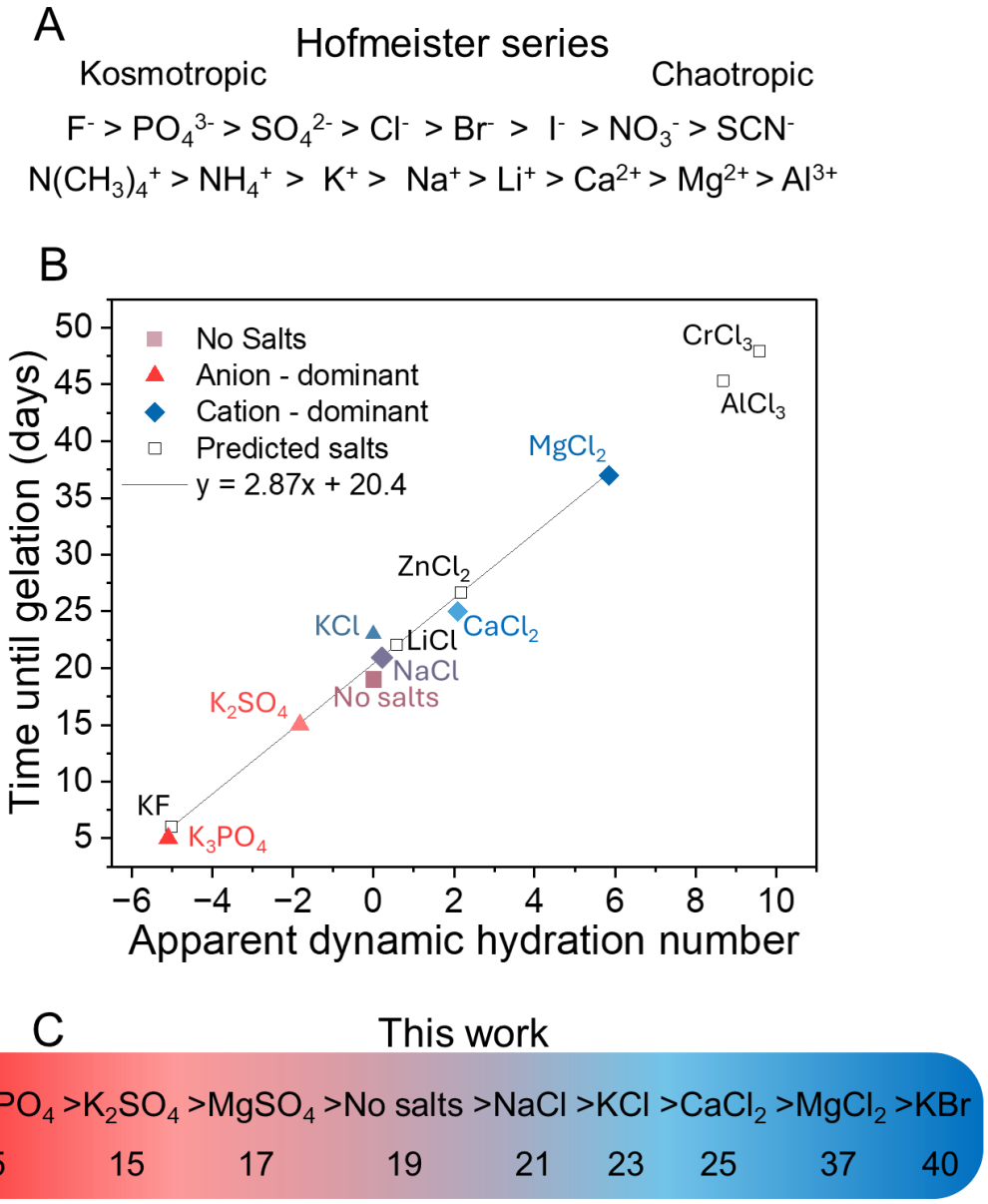

Figure 4. Correlation of silk gelation kinetics. A) Hofmeister series, B) Experimental gelation times of 100 mM salts in 10% RUS plotted against ADHN alongside predicted gelation time of untested salts using trendline obtained from the tested 100mM salts. The trendline is y = 2.87x + 20.4with a R^2=0.98 C) Gelation order assessed in this study, along with the number of days taken for a 10% RUS solution containing 100 mM salts to undergo gelation.

3.4. Speculative role of metal ions in silkworm silk

Having established that within the salt ion pair, anions are the driving force for the silk sol-gel transition, we attempted to update the role of metal ions in native silk fibre spinning (**Figure 5**). Silks aquamelt behaviour would rely significantly on water to orchestrate its self-assembly.[9, 68, 69] In this study, the high correlation between ADHN, which describes a salts affinity to water, and gelation time indicates that the salt alters waters interaction with silk thereby modifying the gelation speed. Traditionally, it is thought that calcium is introduced at the anterior silk gland to help prevent premature gelation and that potassium displaces calcium as silk approaches the spinneret.[3] However, our work has shown that anions are more influential than cations in altering the gelation kinetics. Therefore, it is likely that the anions paired with calcium and potassium within the spinning gland control the sol-gel transition, not just the cations present. We ~~theorise~~ speculate that, like spider silk, chloride anions, alongside divalent cations, may provide stability in the posterior gland while phosphate anions trigger self-assembly into fibres in the anterior gland prior to spinning.[61, 70, 71] Although RUS contains the proteins found in the final spun fibre, it does not fully represent silk as it exists in the gland before spinning. Some proteins, including sericin, are initially partitioned and coat fibroin during spinning, while in RUS, sericin and fibroin are dissolved into a mixed solution. Figure 5 represents an illustration of a theoretical update to the knowledge of ion transport in the spinning gland based on the *in vitro* work presented here. It should be noted that the presence of these anions in the spinning gland have not yet been established and therefore, determining the relative abundance and distribution of anions *in vivo* could offer valuable insights into the role of ionic regulation during silk spinning.

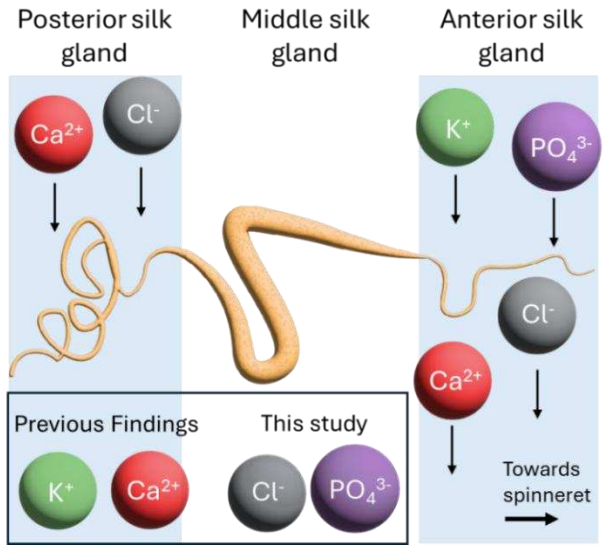

Figure 5. Perspective illustration of a silkworm spinning gland divided into three parts alongside the proposed update to the movement of ions.

4. Conclusion

This study highlights for the first time the critical role that anions play in silkworm silk stabilisation. Like spider silks, monovalent anions such as bromide and chloride were found to significantly stabilise silkworm silk, preventing gelation for more than a month while multivalent anions such as sulphate and phosphate significantly accelerated gelation. Compared with the established role of cations during natural spinning, altering the anion had a more significant effect on gelation, suggesting that anions are more important in driving the sol-gel transition. This work also introduces the apparent dynamic hydration number (ADHN) as a quantitative method to compare the influence of any salt (anion/cation pair) on silk gelation, but might be applicable to other proteins. Overall, the knowledge obtained from this could be used to improve all facets of silk material manufacturing including silk storage, dissolution and the development of controlled coagulation systems for improved artificial spinning and bio printing.

Supporting Information Available

The following files are available free of charge

Zaki et al. Supporting information – Word document containing all supporting graphs and tables.

Acknowledgments

This research was supported in part by the Australian Research Council (IH21000023).

References

(1) Domigan, L. J.; Andersson, M.; Alberti, K. A.; Chesler, M.; Xu, Q.; Johansson, J.; Rising, A.; Kaplan, D. L. Carbonic anhydrase generates a pH gradient in Bombyx mori silk glands. *Insect Biochem Mol Biol* **2015**, *65*, 100-106. DOI: 10.1016/j.ibmb.2015.09.001 From NLM.

(2) Andersson, M.; Chen, G.; Otikovs, M.; Landreh, M.; Nordling, K.; Kronqvist, N.; Westermark, P.; Jörnvall, H.; Knight, S.; Ridderstråle, Y.; et al. Carbonic Anhydrase Generates CO2 and H+ That Drive Spider Silk Formation Via Opposite Effects on the Terminal Domains. *PLOS Biology* **2014**, *12* (8), e1001921. DOI: 10.1371/journal.pbio.1001921.

(3) Zhou, P.; Xie, X.; Knight, D. P.; Zong, X.-H.; Deng, F.; Yao, W.-H. Effects of pH and Calcium Ions on the Conformational Transitions in Silk Fibroin Using 2D Raman Correlation Spectroscopy and 13C Solid-State NMR. *Biochemistry* **2004**, *43* (35), 11302-11311. DOI: 10.1021/bi049344i.

(4) Zhou, L.; Chen, X.; Shao, Z.; Huang, Y.; Knight, D. P. Effect of Metallic Ions on Silk Formation in the Mulberry Silkworm, Bombyx mori. *The Journal of Physical Chemistry B* **2005**, *109* (35), 16937-16945. DOI: 10.1021/jp050883m.

(5) Liu, Q.; Wang, X.; Zhou, Y.; Tan, X.; Xie, X.; Li, Y.; Dong, H.; Tang, Z.; Zhao, P.; Xia, Q. Dynamic Changes and Characterization of the Metal Ions in the Silk Glands and Silk Fibers of Silkworm. *Int J Mol Sci* **2023**, *24* (7). DOI: 10.3390/ijms24076556 From NLM.

(6) Koeppel, A.; Laity, P. R.; Holland, C. The influence of metal ions on native silk rheology. *Acta Biomaterialia* **2020**, *117*, 204-212. DOI: https://doi.org/10.1016/j.actbio.2020.09.045.

(7) Laity, P. R.; Baldwin, E.; Holland, C. Changes in Silk Feedstock Rheology during Cocoon Construction: The Role of Calcium and Potassium Ions. *Macromolecular Bioscience* **2019**, *19* (3), 1800188. DOI: https://doi.org/10.1002/mabi.201800188.
(8) Brookstein, O.; Shimoni, E.; Eliaz, D.; Kaplan-Ashiri, I.; Carmel, I.; Shimanovich, U. Metal ions guide the production of silkworm silk fibers. *Nature Communications* **2024**, *15* (1), 6671. DOI: 10.1038/s41467-024-50879-9.
(9) Laity, P. R.; Holland, C. Seeking Solvation: Exploring the Role of Protein Hydration in Silk Gelation. *Molecules* **2022**, *27* (2), 551.
(10) Laity, P. R.; Gilks, S. E.; Holland, C. Rheological behaviour of native silk feedstocks. *Polymer* **2015**, *67*, 28-39. DOI: https://doi.org/10.1016/j.polymer.2015.04.049.
(11) Schaefer, C.; Laity, P. R.; Holland, C.; McLeish, T. C. B. Stretching of Bombyx mori Silk Protein in Flow. *Molecules* **2021**, *26* (6), 1663.
(12) Zhou, L.; Chen, X.; Shao, Z.; Zhou, P.; Knight, D. P.; Vollrath, F. Copper in the silk formation process of Bombyx mori silkworm. *FEBS Lett* **2003**, *554* (3), 337-341. DOI: 10.1016/s0014-5793(03)01184-0 From NLM.
(13) Brown, K. L.; Banerjee, S.; Feigley, A.; Abe, H.; Blackwell, T. S.; Pozzi, A.; Hudson, B. G.; Zent, R. Salt-bridge modulates differential calcium-mediated ligand binding to integrin α1- and α2-I domains. *Scientific Reports* **2018**, *8* (1), 2916. DOI: 10.1038/s41598-018-21231-1.
(14) Carew, E. B.; Leavis, P. C.; Stanley, H. E.; Gergely, J. A laser Raman spectroscopic study of Ca2+ binding to troponin C. *Biophysical Journal* **1980**, *30* (2), 351-358. DOI: https://doi.org/10.1016/S0006-3495(80)85099-5.
(15) Li, F.; Hu, J.; Tian, J.; Xu, K.; Ni, M.; Wang, B.; Shen, W.; Li, B. Effects of phoxim on nutrient metabolism and insulin signaling pathway in silkworm midgut. *Chemosphere* **2016**, *146*, 478-485. DOI: https://doi.org/10.1016/j.chemosphere.2015.12.032.
(16) Li, F.; Xu, K.; Ni, M.; Wang, B.; Gu, Z.; Shen, W.; Li, B. Effect of oxidative phosphorylation signaling pathway on silkworm midgut following exposure to phoxim. *Environmental Toxicology* **2017**, *32* (1), 167-175. DOI: https://doi.org/10.1002/tox.22222.
(17) Song, J.; Che, J.; You, Z.; Ye, L.; Li, J.; Zhang, Y.; Qian, Q.; Zhong, B. Phosphoproteomic analysis of the posterior silk gland of Bombyx mori provides novel insight into phosphorylation regulating the silk production. *J Proteomics* **2016**, *148*, 194-201. DOI: 10.1016/j.jprot.2016.08.007 From NLM.
(18) Andersson, M.; Johansson, J.; Rising, A. Silk Spinning in Silkworms and Spiders. *Int J Mol Sci* **2016**, *17* (8). DOI: 10.3390/ijms17081290 From NLM.
(19) Yi, Q.; Zhao, P.; Wang, X.; Zou, Y.; Zhong, X.; Wang, C.; Xiang, Z.; Xia, Q.-y. Shotgun proteomic analysis of the Bombyx mori anterior silk gland: An insight into the biosynthetic fiber spinning process. *PROTEOMICS* **2013**, *13* (17), 2657-2663. DOI: https://doi.org/10.1002/pmic.201200443.
(20) Miyake, S.; Azuma, M. Acidification of the Silk Gland Lumen in Bombyx mori and Samia cynthia ricini and Localization of H+-Translocating Vacuolar-Type ATPase. *Journal of Insect Biotechnology and Sericology* **2008**, *77*, 9-16. DOI: 10.11416/jibs.77.1_9.
(21) Kameda, T. Influence of pH, temperature, and concentration on stabilization of aqueous hornet silk solution and fabrication of salt-free materials. *Biopolymers* **2015**, *103* (1), 41-52. DOI: https://doi.org/10.1002/bip.22562.
(22) Song, K.; Wang, Y.; Dong, W.; Li, Z.; He, H.; Zhu, P.; Xia, Q. Silkworm spinning: the programmed self-assembly from natural silk fibroin to superfibre. *bioRxiv* **2021**, 2021.2003.2008.434386. DOI: 10.1101/2021.03.08.434386.
(23) Matsumoto, A.; Chen, J.; Collette, A. L.; Kim, U.-J.; Altman, G. H.; Cebe, P.; Kaplan, D. L. Mechanisms of Silk Fibroin Sol−Gel Transitions. *The Journal of Physical Chemistry B* **2006**, *110* (43), 21630-21638. DOI: 10.1021/jp056350v.
(24) Miali, M. E.; Eliaz, D.; Solomonov, A.; Shimanovich, U. Microcompartmentalization Controls Silk Feedstock Rheology. *Langmuir* **2023**, *39* (26), 8984-8995. DOI: 10.1021/acs.langmuir.3c00354.
(25) Hofmeister, F. Zur Lehre von der Wirkung der Salze. *Archiv für experimentelle Pathologie und Pharmakologie* **1888**, *24* (4), 247-260. DOI: 10.1007/BF01918191.

(26) Zhang, Y.; Furyk, S.; Bergbreiter, D. E.; Cremer, P. S. Specific Ion Effects on the Water Solubility of Macromolecules: PNIPAM and the Hofmeister Series. *Journal of the American Chemical Society* **2005**, *127* (41), 14505-14510. DOI: 10.1021/ja0546424.
(27) Gregory, K. P.; Elliott, G. R.; Robertson, H.; Kumar, A.; Wanless, E. J.; Webber, G. B.; Craig, V. S. J.; Andersson, G. G.; Page, A. J. Understanding specific ion effects and the Hofmeister series. *Physical Chemistry Chemical Physics* **2022**, *24* (21), 12682-12718, 10.1039/D2CP00847E. DOI: 10.1039/D2CP00847E.
(28) Yang, Z. Hofmeister effects: an explanation for the impact of ionic liquids on biocatalysis. *Journal of Biotechnology* **2009**, *144* (1), 12-22. DOI: https://doi.org/10.1016/j.jbiotec.2009.04.011.
(29) Pegram, L. M.; Record, M. T. Hofmeister Salt Effects on Surface Tension Arise from Partitioning of Anions and Cations between Bulk Water and the Air−Water Interface. *The Journal of Physical Chemistry B* **2007**, *111* (19), 5411-5417. DOI: 10.1021/jp070245z.
(30) Zhang, Y.; Cremer, P. S. The inverse and direct Hofmeister series for lysozyme. *Proc Natl Acad Sci U S A* **2009**, *106* (36), 15249-15253. DOI: 10.1073/pnas.0907616106 From NLM.
(31) Mohammadi, P.; Jonkergouw, C.; Beaune, G.; Engelhardt, P.; Kamada, A.; Timonen, J. V. I.; Knowles, T. P. J.; Penttila, M.; Linder, M. B. Controllable coacervation of recombinantly produced spider silk protein using kosmotropic salts. *Journal of Colloid and Interface Science* **2020**, *560*, 149-160. DOI: https://doi.org/10.1016/j.jcis.2019.10.058.
(32) Leclerc, J.; Lefèvre, T.; Gauthier, M.; Gagné, S. M.; Auger, M. Hydrodynamical properties of recombinant spider silk proteins: Effects of pH, salts and shear, and implications for the spinning process. *Biopolymers* **2013**, *99* (9), 582-593. DOI: 10.1002/bip.22218 From NLM.
(33) Wen, F.; Wang, Y.; Tu, B.; Cui, L. Superfast Gelation of Spider Silk-Based Artificial Silk Protein. *Gels* **2024**, *10* (1), 69.
(34) Zhang, Y.; Zhao, P.; Dong, Z.; Wang, D.; Guo, P.; Guo, X.; Song, Q.; Zhang, W.; Xia, Q. Comparative Proteome Analysis of Multi-Layer Cocoon of the Silkworm, Bombyx mori. *PLOS ONE* **2015**, *10* (4), e0123403. DOI: 10.1371/journal.pone.0123403.
(35) Zaki, M.; Rajkhowa, R.; Holland, C.; Razal, J. M.; Hegh, D. Y.; Mota-Santiago, P.; Lynch, P.; Allardyce, B. J. Recreating Silk's Fibrillar Nanostructure by Spinning Solubilized, Undegummed Silk (Adv. Mater. 15/2025). *Advanced Materials* **2025**, *37* (15), 2570115. DOI: https://doi.org/10.1002/adma.202570115.
(36) Allardyce, B. J.; Rajkhowa, R.; Dilley, R. J.; Atlas, M. D.; Kaur, J.; Wang, X. The impact of degumming conditions on the properties of silk films for biomedical applications. *Textile Research Journal* **2016**, *86* (3), 275-287. DOI: 10.1177/0040517515586166.
(37) Yao, Y.; Allardyce, B. J.; Rajkhowa, R.; Guo, C.; Mu, X.; Hegh, D.; Zhang, J.; Lynch, P.; Wang, X.; Kaplan, D. L.; Razal, J. M. Spinning Regenerated Silk Fibers with Improved Toughness by Plasticizing with Low Molecular Weight Silk. *Biomacromolecules* **2021**, *22* (2), 788-799. DOI: 10.1021/acs.biomac.0c01545.
(38) Boulet-Audet, M.; Holland, C.; Gheysens, T.; Vollrath, F. Dry-Spun Silk Produces Native-Like Fibroin Solutions. *Biomacromolecules* **2016**, *17* (10), 3198-3204. DOI: 10.1021/acs.biomac.6b00887.
(39) Percot, A.; Colomban, P.; Paris, C.; Dinh, H. M.; Wojcieszak, M.; Mauchamp, B. Water dependent structural changes of silk from Bombyx mori gland to fibre as evidenced by Raman and IR spectroscopies. *Vibrational Spectroscopy* **2014**, *73*, 79-89. DOI: https://doi.org/10.1016/j.vibspec.2014.05.004.
(40) Laemmli, U. K. Cleavage of Structural Proteins during the Assembly of the Head of Bacteriophage T4. *Nature* **1970**, *227* (5259), 680-685. DOI: 10.1038/227680a0.
(41) Kurien, B. T.; Scofield, R. H. Common artifacts and mistakes made in electrophoresis. *Methods Mol Biol* **2012**, *869*, 633-640. DOI: 10.1007/978-1-61779-821-4_58 From NLM.
(42) *Gel Molecular Weight Analyzer*; Origin: 2019. https://www.originlab.com/fileExchange/details.aspx?fid=522 (accessed.

(43) Kalita, M.; Allardyce, B. J.; Sankaranarayanan, K.; Devi, D.; Rajkhowa, R. Sericin from mulberry and non-mulberry silk using chemical-free degumming. *The Journal of The Textile Institute* **2022**, *113* (10), 2080-2089. DOI: 10.1080/00405000.2021.1964766.
(44) Koshy, D. S.; Allardyce, B. J.; Dumée, L. F.; Suttib, A.; Rajkhowab, R.; Agrawala, R. Enhancing the reusability and peroxidase-like activity of copper/sericin hybrid nanoflowers by controlling protein molecular weight. *ACS Applied Materials & Interfaces* **2023**.
(45) Schaefer, C.; Laity, P. R.; Holland, C.; McLeish, T. C. B. Silk Protein Solution: A Natural Example of Sticky Reptation. *Macromolecules* **2020**, *53* (7), 2669-2676. DOI: 10.1021/acs.macromol.9b02630.
(46) Schaefer, C.; McLeish, T. C. B. Theoretical rheo-physics of silk: Intermolecular associations reduce the critical specific work for flow-induced crystallization. *Journal of Rheology* **2022**, *66* (3), 515-534. DOI: 10.1122/8.0000411 (acccessed 12/19/2024).
(47) Heuer, J.; Kraus, Y.; Vučak, M.; Zeng, A. P. Enhanced sequestration of carbon dioxide into calcium carbonate using pressure and a carbonic anhydrase from alkaliphilic Coleofasciculus chthonoplastes. *Eng Life Sci* **2022**, *22* (3-4), 178-191. DOI: 10.1002/elsc.202100033 From NLM.
(48) Wang, X.; Kluge, J. A.; Leisk, G. G.; Kaplan, D. L. Sonication-induced gelation of silk fibroin for cell encapsulation. *Biomaterials* **2008**, *29* (8), 1054-1064. DOI: 10.1016/j.biomaterials.2007.11.003 From NLM.
(49) Dubey, P.; Seit, S.; Chowdhury, P. K.; Ghosh, S. Effect of Macromolecular Crowders on the Self-Assembly Process of Silk Fibroin. *Macromolecular Chemistry and Physics* **2020**, *221* (16), 2000113. DOI: https://doi.org/10.1002/macp.202000113.
(50) Humenik, M.; Smith, A. M.; Arndt, S.; Scheibel, T. Ion and seed dependent fibril assembly of a spidroin core domain. *Journal of Structural Biology* **2015**, *191* (2), 130-138. DOI: https://doi.org/10.1016/j.jsb.2015.06.021.
(51) Kamada, A.; Toprakcioglu, Z.; Knowles, T. P. J. Kinetic Analysis Reveals the Role of Secondary Nucleation in Regenerated Silk Fibroin Self-Assembly. *Biomacromolecules* **2023**, *24* (4), 1709-1716. DOI: 10.1021/acs.biomac.2c01479.
(52) Martineau, R. L.; Bayles, A. V.; Hung, C.-S.; Reyes, K. G.; Helgeson, M. E.; Gupta, M. K. Engineering Gelation Kinetics in Living Silk Hydrogels by Differential Dynamic Microscopy Microrheology and Machine Learning. *Advanced Biology* **2022**, *6* (1), 2101070. DOI: https://doi.org/10.1002/adbi.202101070.
(53) Ribeiro, V. P.; Silva-Correia, J.; Gonçalves, C.; Pina, S.; Radhouani, H.; Montonen, T.; Hyttinen, J.; Roy, A.; Oliveira, A. L.; Reis, R. L.; Oliveira, J. M. Rapidly responsive silk fibroin hydrogels as an artificial matrix for the programmed tumor cells death. *PLoS One* **2018**, *13* (4), e0194441. DOI: 10.1371/journal.pone.0194441 From NLM.
(54) Kwak, H. W.; Ju, J. E.; Shin, M.; Holland, C.; Lee, K. H. Sericin Promotes Fibroin Silk I Stabilization Across a Phase-Separation. *Biomacromolecules* **2017**, *18* (8), 2343-2349. DOI: 10.1021/acs.biomac.7b00549.
(55) Geisler, M.; Pirzer, T.; Ackerschott, C.; Lud, S.; Garrido, J.; Scheibel, T.; Hugel, T. Hydrophobic and Hofmeister effects on the adhesion of spider silk proteins onto solid substrates: an AFM-based single-molecule study. *Langmuir* **2008**, *24* (4), 1350-1355. DOI: 10.1021/la702341j From NLM.
(56) Wigham, C.; Varude, V.; O'Donnell, H.; Zha, R. H. The role of phosphate in silk fibroin self-assembly: a Hofmeister study. *Soft Matter* **2025**, *21* (13), 2461-2470, 10.1039/D4SM01198H. DOI: 10.1039/D4SM01198H.
(57) Li, F.; Li, J.; Huang, G.; Wang, W.; Dong, W.; Yan, L. Surface Activity Study of Water-Soluble Silk Fibroin Prepared using Cocoons and Ca(NO3)2 · 4H2O. *Tenside Surfactants Detergents* **2017**, *54* (4), 299-307. DOI: doi:10.3139/113.110512 (acccessed 2024-09-04).
(58) Yamada, H.; Nakao, H.; Takasu, Y.; Tsubouchi, K. Preparation of undegraded native molecular fibroin solution from silkworm cocoons. *Materials Science and Engineering: C* **2001**, *14* (1), 41-46. DOI: https://doi.org/10.1016/S0928-4931(01)00207-7.
(59) Yao, Y.; Allardyce, B. J.; Rajkhowa, R.; Hegh, D.; Sutti, A.; Subianto, S.; Gupta, S.; Rana, S.; Greenhill, S.; Venkatesh, S.; et al. Improving the Tensile Properties of Wet Spun Silk Fibers Using Rapid Bayesian

Algorithm. *ACS Biomaterials Science & Engineering* **2020**, *6* (5), 3197-3207. DOI: 10.1021/acsbiomaterials.0c00156.
(60) Schmuck, B.; Greco, G.; Bäcklund, F. G.; Pugno, N. M.; Johansson, J.; Rising, A. Impact of physio-chemical spinning conditions on the mechanical properties of biomimetic spider silk fibers. *Communications Materials* **2022**, *3* (1), 83. DOI: 10.1038/s43246-022-00307-6.
(61) Eisoldt, L.; Smith, A.; Scheibel, T. Decoding the secrets of spider silk. *Materials Today* **2011**, *14* (3), 80-86. DOI: https://doi.org/10.1016/S1369-7021(11)70057-8.
(62) Kiriukhin, M. Y.; Collins, K. D. Dynamic hydration numbers for biologically important ions. *Biophysical Chemistry* **2002**, *99* (2), 155-168. DOI: https://doi.org/10.1016/S0301-4622(02)00153-9.
(63) Collins, K. D. The behavior of ions in water is controlled by their water affinity. *Quarterly Reviews of Biophysics* **2019**, *52*, e11. DOI: 10.1017/S0033583519000106 From Cambridge University Press Cambridge Core.
(64) Slavchov, R. I.; Peychev, B.; Minkov, I. Electrolytes at Uncharged Liquid Interfaces: Adsorption, Potentials, Surface Tension, and the Role of the Surfactant Monolayer. *Langmuir* **2024**, *40* (33), 17170-17189. DOI: 10.1021/acs.langmuir.4c01388.
(65) Collins, K. D. Ions from the Hofmeister series and osmolytes: effects on proteins in solution and in the crystallization process. *Methods* **2004**, *34* (3), 300-311. DOI: https://doi.org/10.1016/j.ymeth.2004.03.021.
(66) Jin, H.-J.; Kaplan, D. L. Mechanism of silk processing in insects and spiders. *Nature* **2003**, *424* (6952), 1057-1061. DOI: 10.1038/nature01809.
(67) Yao, Y.; Allardyce, B. J.; Rajkhowa, R.; Hegh, D.; Qin, S.; Usman, K. A. S.; Mota-Santiago, P.; Zhang, J.; Lynch, P.; Wang, X.; et al. Toughening Wet-Spun Silk Fibers by Silk Nanofiber Templating. *Macromolecular Rapid Communications* **2022**, *43* (7), 2100891. DOI: https://doi.org/10.1002/marc.202100891.
(68) Holland, C.; Vollrath, F.; Ryan, A. J.; Mykhaylyk, O. O. Silk and Synthetic Polymers: Reconciling 100 Degrees of Separation. *Advanced Materials* **2012**, *24* (1), 105-109. DOI: https://doi.org/10.1002/adma.201103664.
(69) Porter, D.; Vollrath, F. Water mobility, denaturation and the glass transition in proteins. *Biochim Biophys Acta* **2012**, *1824* (6), 785-791. DOI: 10.1016/j.bbapap.2012.03.007 From NLM.
(70) Malay, A. D.; Suzuki, T.; Katashima, T.; Kono, N.; Arakawa, K.; Numata, K. Spider silk self-assembly via modular liquid-liquid phase separation and nanofibrillation. *Science Advances* **2020**, *6* (45), eabb6030. DOI: doi:10.1126/sciadv.abb6030.
(71) Fan, R.; Knuuttila, K.; Schmuck, B.; Greco, G.; Rising, A.; Linder, M. B.; Aranko, A. S. Sustainable Spinning of Artificial Spider Silk Fibers with Excellent Toughness and Inherent Potential for Functionalization. *Advanced Functional Materials* **2024**, *n/a* (n/a), 2410415. DOI: https://doi.org/10.1002/adfm.202410415 (acccessed 2024/08/20).